In: Cell Membrane
Editors: L. Mandraccia and G. Slavin
ISBN: 978-1-62808-456-6

Chapter 3

Effects of Surface Charge and Particle Size of Cell-Penetrating Peptide/Nanoparticle Complexes on Cellular Internalization

Betty Revon Liu,[1] Ming-Huan Chan,[2]
Hwei-Hsien Chen,[3] Shih-Yen Lo,[4]
Yue-Wern Huang[5] and Han-Jung Lee[1,*]
[1]Department of Natural Resources and Environmental Studies,
National Dong Hwa University, Hualien, Taiwan
[2]Institute of Neuroscience, National Chengchi University,
Taipei, Taiwan
[3]Institute of Population Health Sciences,
National Health Research Institutes, Miaoli, Taiwan
[4]Department of Laboratory Medicine and Biotechnology,
Tzu Chi University, Hualien, Taiwan
[5]Department of Biological Sciences,
Missouri University of Science and Technology, Rolla, MO, US

[*] Corresponding author: Han-Jung Lee. E-mail: hjlee@mail.ndhu.edu.tw.

Abstract

Cell membranes are natural barriers that prevent macromolecules from permeating cells. The efficiency of exogenous materials entering cells relies on various strategies and factors. Cell-penetrating peptides (CPPs) are distinctive molecules that can penetrate cells by themselves, as well as carry cargoes into cells in both covalent and noncovalent manners. In this chapter, we use CPP-mediated delivery of nanomaterials to illustrate the importance of surface charge and size of nanoparticles on cellular uptake. We found that three different arginine-rich CPPs (SR9, HR9, and PR9) are able to form stable complexes with nanomaterials, including quantum dots (QDs) and DNAs, and the complexes can effectively internalize into cells. Our study demonstrated that zeta-potential of CPP/cargo nanoparticulate complexes is a key predictor of transduction efficiency. On a different note, a combination of CPPs with cargoes resulted in complexes with various sizes. The most positively charged HR9/cargo complexes displayed the highest protein transduction efficiency. The correlation coefficient analysis demonstrated a high correlation between zeta-potential and transduction efficiency of CPP/DNA complexes. A logarithmic curve was plotted with zeta value against transduction efficiency with an R-squared value of 0.9454. With similar surface charges, particle sizes could affect cellular uptake efficiency of CPP/QD complexes. Collectively, our findings elucidate that zeta-potential of CPP/cargo nanoparticulate complexes plays a major role in determining transduction efficiency, while particle sizes of CPP/cargo nanoparticulate complexes have a minor effect in cell permeability.

Abbreviations

CPP	cell-penetrating peptide
GFP	green fluorescent protein
EGFP	enhanced green fluorescent protein
HR9	histidine-rich nona-arginine
N/P	nitrogen (NH_3^+)/phosphate (PO_4^-)
PR9	Pas nona-arginine
PTD	protein transduction domain
QD	quantum dot
SR9	synthetic nona-arginine
Tat	transactivator of transcription

Introduction

The plasma membrane plays an essential role in selective permeability, compartmentalization, osmotic balance, and cellular uptake. Understanding of mechanisms and principles organizing thousands of proteins and lipids that make up cellular membrane bilayers is still incomplete [1]. Small molecules, such as ions, sugars, and amino acids, are able to permeate cells through carriers and channels on the membrane. This mode of entry is generally not available for macromolecules, such as proteins, DNAs, and RNAs. In order to develop highly efficient strategies for the controlled cellular delivery of bioactive macromolecules with therapeutic potential, several non-viral carrier systems, including liposomes, polycationic carriers, nanomaterials, and peptides, have been developed.

Cell-penetrating peptides (CPPs) are typically short peptides that are derived from natural, chimeric, and synthetic sources [2, 3]. The first CPP discovered is a protein transduction domain (PTD) derived from the transactivator of transcription (Tat) of the human immunodeficiency virus type 1 (HIV-1) [4, 5]. This PTD containing eleven amino acids (YGRKKRR-QRRR) is responsible for cellular entry of Tat [6]. CPPs include cationic, amphipathic, and hydrophobic peptides [3]. CPPs have been used to overcome the lipophilic barrier of cellular membranes and to deliver exogenous molecules into the cell for various purposes, such as cellular imaging, biosensing, or molecular delivery [7]. These peptides can translocate through biological membranes and facilitate efficient delivery of cargoes into living cells or organisms. Cargoes can be proteins [8–19], DNAs [20–26], RNAs [27], liposomes [28, 29], and inorganic nanoparticles [30–38]. CPPs can deliver cargoes with sizes up to 200 nm in diameter [28, 29]. Despite many studies using various biological and biophysical techniques, our understanding of cellular uptake mechanisms of CPPs remains incomplete. Previous studies have indicated that CPPs enter cells by at least two major routes, energy-independent direct membrane translocation and energy-dependent endocytosis, or a combination of multiple pathways [2]. As membrane potential has a crucial role in cellular internalization of arginine-rich CPPs [39–41], zeta-potentials of CPP/cargo complexes can influence transduction efficiency. In this chapter, we selected CdSe/ZnS quantum dots (QDs) and DNAs to investigate the role of zeta-potential in protein transduction. QDs are colloidal nano-sized semiconductors with unique chemical, physical, and optical properties [42], such as photostability, high quantum yield, narrow emission peak, resistance to degradation, and broad size-dependent photoluminescence

[43]. These nanoparticles have been used in various bioimaging and diagnostic applications [30–38, 44]. Zeta-potential of these nanoparticles varies depending on particle size, methods of production and treatment, surface structure, and other properties [40, 45]. The effects of zeta-potential and size of CPP/cargo complexes can give insight into the stability of particles in solution [46, 47].

Materials and Methods

Cell Culture

Human A549 lung cancer cells (American Type Culture Collection, Manassas, VA, US; CCL-185) were maintained in Roswell Park Memorial Institute (RPMI) 1640 medium supplemented with 10% (v/v) fetal bovine serum (Gibco, Invitrogen, Carlsbad, CA, US), as previously described [9].

Peptide, Nanoparticle, and Plasmid Preparation

Three arginine-rich CPPs, synthetic nona-arginine (SR9; RRRRRRRRR), histidine-rich nona-arginine (HR9; CHHHHHRRRRRRRRRHHHHHC), and Pas nona-arginine (PR9; FFLIPKGRRRRRRRRR), were synthesized as previously described [21, 37]. CdSe/ZnS QDs with the maximal emission peak wavelength of 525 nm (carboxyl-functionalized eFluor 525NC) were purchased from eBioscience (San Diego, CA, US). The pEGFP-N1 plasmid contains the enhanced green fluorescent protein (*EGFP*) coding sequence under the control of the cytomegalovirus (CMV) promoter (Clontech, Mountain View, CA, US). The pBacCecB-EGFP plasmid consists of the insect EGFP cassette which includes the strong *cecropin B1* (*CecB*) gene promoter of silkworm, coding region of *EGFP*, and *3'CecB* region [23].

Noncovalent Protein Transduction

In noncovalent protein transduction, cells were treated with QDs, DNAs or CPP/cargo complexes, as previously described [24, 33].

Six μM of CPP peptide was mixed with 100 nM of QDs at a molecular ratio of 60 at 37°C for 2 h. CPP/QD complexes were then incubated with cells

at 37°C for 1 h followed by analyses using a fluorescent microscope, a flow cytometer, or a Zetasizer. Three μg of the pEGFP-N1 or pBacCecB-EGFP plasmid DNA served as a control, or CPPs were mixed with plasmid DNAs at a nitrogen (NH3+)/phosphate (PO4–) (N/P) ratio of 3. Cells were treated with DNA alone or CPP/DNA complexes for 48 h and then analyzed using a confocal microscope.

Confocal and Fluorescent Microscopy

Fluorescent and bright-field images were obtained using Olympus IX70 and IX71 inverted fluorescent microscopes (Olympus, Center Valley, PA, US), as previously described [15]. For the green fluorescent protein (GFP) detection, excitation was at 460–490 nm, and emission was at 520 nm.

Confocal images were recorded using a BD Pathway 435 System (BD Biosciences, Franklin Lakes, NJ, US), as previously described [33]. For the GFP detection, excitation was at 482/35 nm, and emission was at 536/40 nm. The transduction efficiency were determined from the digital image data and analyzed by UN-SCAN-IT software (Silk Scientific, Orem, UT, US).

Zeta-Potential Analysis and Particle Size Measurement

QDs (100 nM), DNAs (3 μg) or CPP/cargo complexes were dissolved in distilled and deionized water. Each solution was equilibrated at 25°C for 120 sec in a zeta cell. Zeta-potentials and particle sizes of QDs, DNAs, and CPP/cargo complexes were analyzed using a Zetasizer Nano ZS (Malvern Instruments, Worcestershire, UK) and Zetasizer software 6.30 [40].

Flow Cytometry

Flow cytometric analysis was conducted as previously described [13]. CPP/QD complexes-treated cells were analyzed using a Cytomics FC500 flow cytometer (Beckman Coulter, Fullerton, CA, US). FL1 filter (excitation at 488 nm and emission at 525 nm) was used for GFP detection. Results were then analyzed using CXP software (Beckman Coulter).

Statistical Analysis

Results are expressed as mean ± standard deviation. Mean values and standard deviations were calculated from at least three independent experiments carried out in triplicates per treatment group.

Results

CPP/QD complexes were chosen for noncovalent protein transduction in human A549 cells. QDs were pre-mixed without or with CPPs (including SR9, HR9, and PR9) and then added to cells for 1 h. Fluorescent microscopy showed no detectable signal in the cells treated with QDs alone (Figure 1). In contrast, green fluorescence was observed in the cells treated with SR9/QD, HR9/QD, and PR9/QD complexes. These results indicate that CPP/QD nanoparticulate complexes have the abilities to pass through cell membranes and enter cells.

To investigate physicochemical properties of CPP/QD nanoparticulate complexes that influence transduction efficiency, we measured cellular internalization efficiencies, sizes, and zeta-potentials of CPP/QD complexes.

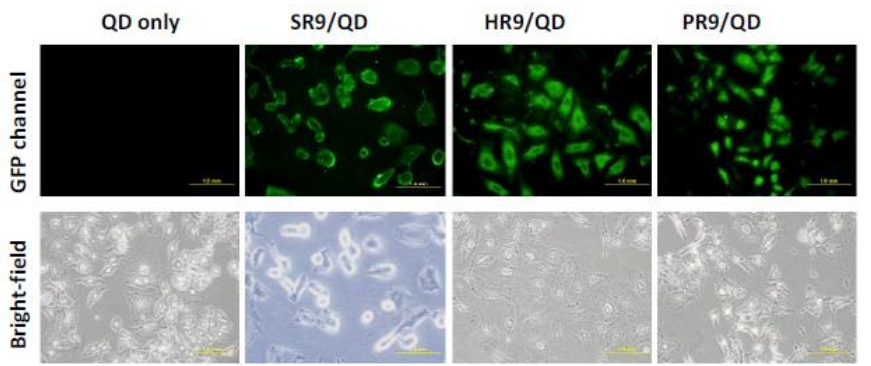

Figure 1. CPP-mediated QD delivery in A549 cells. QDs were incubated with SR9, HR9, and PR9 for 2 h, respectively. Cells were treated with QDs alone or these complexes for 1 h and then observed using a fluorescent microscope. GFP channel indicated the intracellular distribution of QDs. Cell morphology was shown in bright-field images. Images were recorded at a magnification of 400× using Olympus IX70 (SR9/QD complexes) and IX71 (QD only, HR9/QD, and PR9/QD complexes) inverted fluorescent microscopes. Scale bar is 1.0 μm.

Cells were treated with QDs alone or CPP/QD complexes and analyzed by flow cytometry. Sizes and zeta-potentials of QDs alone or CPP/QD complexes were determined using a Zetasizer. The fraction of the cell population with the complexes was in the order of HR9/QD＞PR9/QD≧SR9/QD complexes (Figure 2a). QDs alone were 2.01 ± 0.14 nm in diameter. Three different CPP/QD complexes exhibited a similar size of 15.69 ± 1.10 nm in diameter. Zeta-potentials of CPP/QD complexes were more electropositive than that of QDs, and were in the same order as transduction efficiencies of HR9/QD＞PR9/QD≧SR9/QD complexes (Figure 2b). These results suggest that a more electropositive charge of CPP/QD complexes yields a relatively higher transduction efficiency.

To further investigate whether charge and size effects are cargo-specific, we incubated CPPs with DNAs to perform a functional gene assay. The transduced pEGFP-N1 plasmid DNA could be expressed by cells to serve as an indication of CPP-transduction efficiency. The population of EGFP-expressing cells was in the order of HR9/DNA＞PR9/DNA≧SR9/DNA complexes, similar to that of QD cargo (Figure 3a). However, particle size was in a different order of SR9/DNA≧PR9/DNA＞HR9/DNA complexes. Zeta-potentials of CPP/DNA complexes were more electropositive than that of DNAs, and were in the same order as transduction efficiencies of HR9/DNA＞PR9/DNA≧SR9/DNA complexes (Figure 3b).

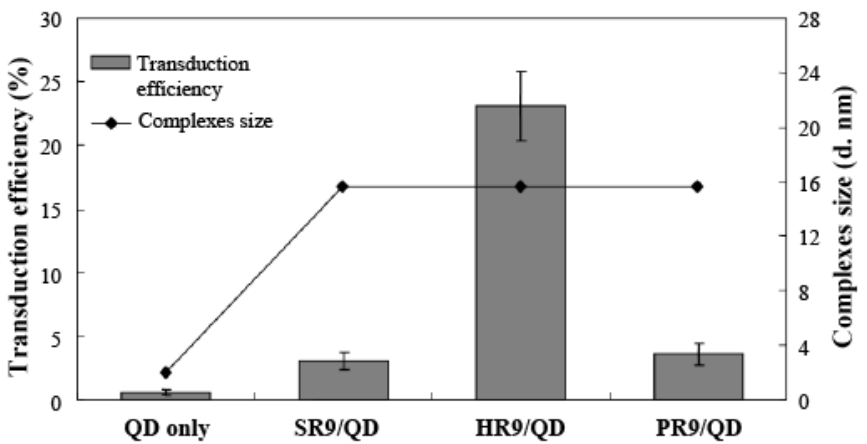

a

Figure 2. (Continued).

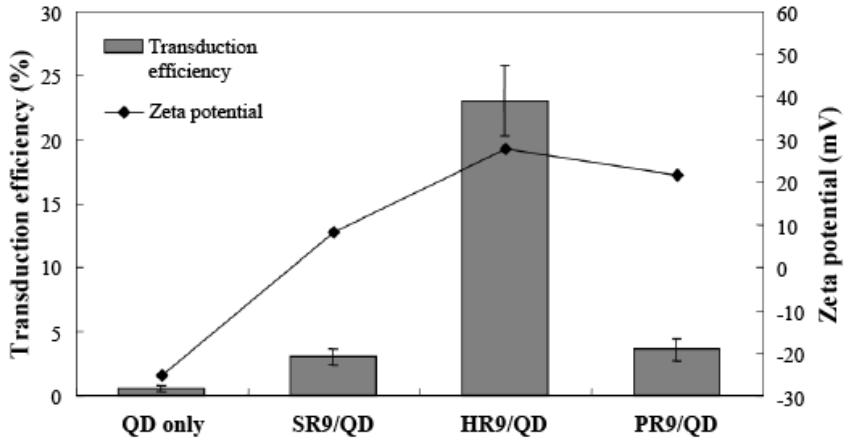

b

Figure 2. Comparison between transduction efficiencies and physicochemical properties of CPP/QD nanoparticulate complexes. (a) Transduction efficiency versus size of CPP/QD complexes. SR9, HR9, and PR9 were mixed with QDs at a molecular ratio of 60 and then incubated with A549 cells. The sizes of the complexes were measured using a Zetasizer (at the right y-axis). The fraction of fluorescent cell population was detected by flow cytometry regarding as the transduction efficiency of QDs mediated by CPPs (at the left y-axis). (b) Transduction efficiency versus zeta-potential of CPP/QD complexes. Zeta-potentials of CPP/QD complexes were measured using a Zetasizer. Data of transduction efficiency are presented as mean ± standard deviation from 27 independent experiments carried out in triplicates per treatment group.

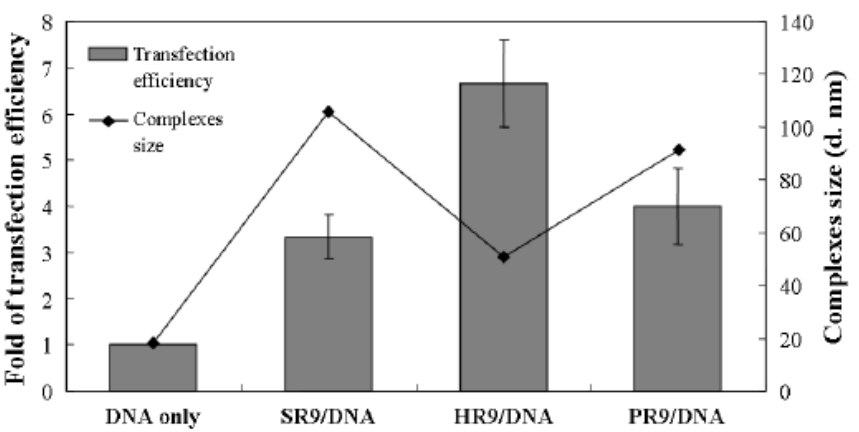

a

Figure 3. (Continued).

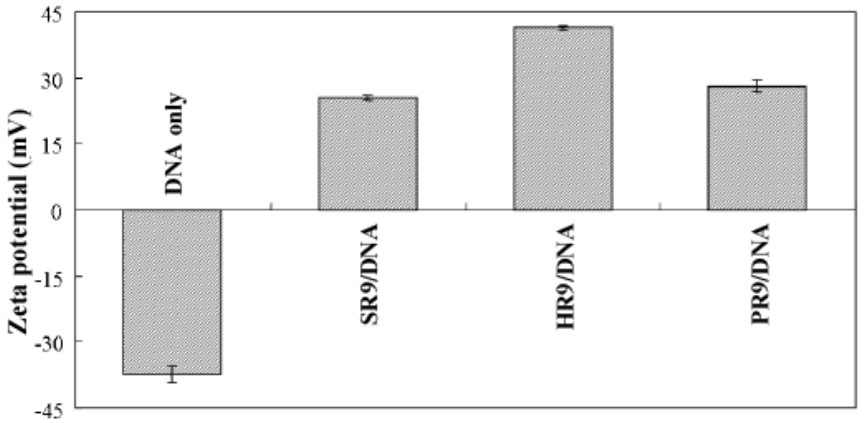

b

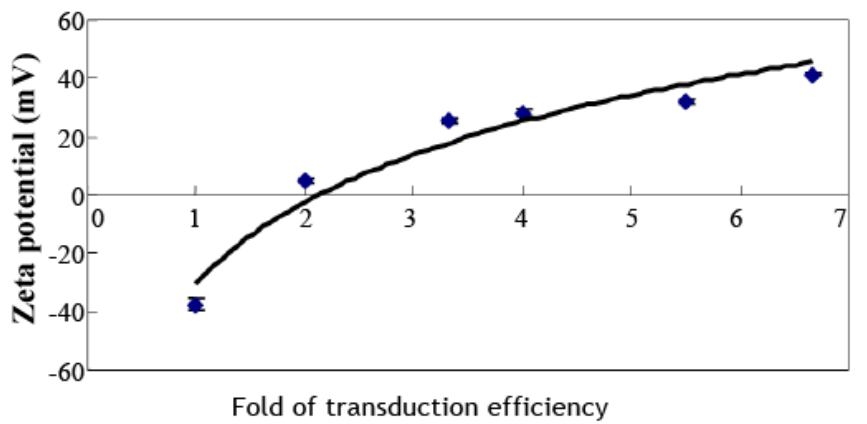

c

Figure 3. Comparison between transduction efficiencies and physicochemical properties of CPP/DNA nanoparticulate complexes. (a) Transduction efficiency *versus* size of CPP/DNA complexes. pEGFP-N1 plasmid DNAs were incubated with SR9, HR9, and PR9 at an N/P ratio of 3. Sizes of the complexes were analyzed using a Zetasizer. A549 cells were treated with pEGFP-N1 (DNAs) alone or different CPP/DNA complexes. Cell images of gene expression were taken in GFP channel using a BD pathway system. Data of transduction efficiency are presented as mean ± standard deviation from 3 independent experiments carried out in triplicates per treatment group. (b) Zeta-potentials of different CPP/DNA complexes. CPPs were mixed with pBacCecB-EGFP plasmid DNAs according to above conditions. Zeta-potential of different CPP/DNA complexes is represented by mean ± standard deviation from 3 independent experiments carried out in triplicates per treatment group. (c) A logarithmic curve plotted with fold of transduction efficiency against zeta-potential.

The correlation coefficient analysis demonstrated a high correlation between zeta-potential and transduction efficiency of CPP/DNA complexes (Figure 3c).

A logarithmic curve showed a high correlation ($R^2 = 0.9454$) between zeta value and transduction efficiency. Collectively, these results indicate that zeta-potentials of CPP/cargo complexes can be used as a predictor of transduction efficiencies of CPP/cargo complexes.

Discussion

In this chapter, we demonstrate the effects of charge and size of CPP/cargo nanoparticulate complexes on cellular uptake efficiency. Three arginine-rich CPPs (SR9, HR9, and PR9) were able to deliver noncovalently associated nanomaterials, including QDs and DNAs, into living cells. There was a high correlation between zeta-potential and protein transduction efficiency of CPP/cargo complexes. We conclude that zeta-potentials of CPP/nanoparticle complexes play a major role in determining transduction efficiency.

Zeta-potential represents an electrokinetic potential in colloidal systems. Both zeta-potential and particle size distribution are fundamental to predict the stability and rheology of colloidal suspensions [48, 49]. In general, electropositivity at or above 25 mV is used as an arbitrary threshold of low- or highly-charged surfaces, that contributes to suspension stability in colloidal systems [50].

The stability of aqueous particle dispersions requires zeta-potentials greater than ± 30 mV [51]. Carboxyl-functionalized QDs and plasmid DNA have intrinsic negative zeta values. Hence, the increase in zeta-potentials contributed by positively charged CPPs facilitates electrostatic interactions of CPP/QD and CPP/DNA nanoparticulate complexes with plasma membranes, leading to better cellular internalization.

We recently identified several factors that determine the mechanism of CPPs entry [18]. Three arginine-rich CPPs (R9, SR9 and HR9) were studied in human, plant, and bacterial cells. Pharmacological and physical treatments were used to elucidate the nature of the transport mechanisms. The route of internalization is relatively unaffected by cell type, but is heavily dependent on the nature of both CPPs and associated cargoes.

Conclusion

In this chapter, we demonstrate that three arginine-rich CPPs (SR9, HR9, and PR9) are able to deliver noncovalently associated QDs and DNAs into cells. The sizes of CPP/cargo nanoparticulate complexes seem not an effective predictor of transduction efficiency. In contrast, a significant correlation between zeta-potential and transduction efficiency was identified. This highlights the importance of electrostatic property that governs interactions of CPP/cargo complexes with negatively charged plasma membranes. The outcome of the interactions is a key factor in determining transduction efficiency. Thus, zeta-potential of CPP/cargo complexes is a key predictor of transduction efficiency.

Acknowledgments

We thank Dr. Chia-Liang Cheng (Department of Physics, National Dong Hwa University, Taiwan) for performing the zeta-potential measurements. This work was supported by the Postdoctoral Fellowship NSC 101-2811-B-259-001 (to B.R.L.) and the Grant Number NSC 101-2320-B-259-002-MY3 (to H.-J.L.) from the National Science Council, Taiwan.

References

[1] Mueller, N. S., Wedlich-Soldner, R. and Spira, F. (2012). From mosaic to patchwork: matching lipids and proteins in membrane organization. *Mol. Membr. Biol*., 25, 186–196.

[2] Madani, F., Lindberg, S., Langel, U., Futaki, S., and Graslund, A. (2011). Mechanisms of cellular uptake of cell-penetrating peptides. *J. Biophys*., 2011, 414729.

[3] Wagstff, K. M. and Jans, D. A. (2006). Protein transduction: cell penetrating peptides and their therapeutic applications. *Curr. Med. Chem*., 13, 1371–1387.

[4] Green, M. and Loewenstein, P. M. (1988). Autonomous functional domains of chemically synthesized human immunodeficiency virus Tat trans-activator protein. *Cell*, 55, 1179–1188.

[5] Frankel, A. D. and Pabo, C. O. (1988). Cellular uptake of the tat protein from human immunodeficiency virus. *Cell*, 55, 1189–1193.

[6] Vives, E., Brodin, P. and Lebleu, B. (1997). A truncated HIV-1 Tat protein basic domain rapidly translocates through the plasma membrane and accumulates in the cell nucleus. *J. Biol. Chem.*, 272, 16010–16017.

[7] Pavan, S. and Berti, F. (2012). Short peptides as biosensor transducers. *Anal. Bioanal. Chem*., 402, 3055–3070.

[8] Chang, M., Chou, J. C. and Lee, H. J. (2005). Cellular internalization of fluorescent proteins via arginine-rich intracellular delivery peptide in plant cells. *Plant Cell Physiol*., 46, 482–488.

[9] Wang, Y. H., Chen, C. P., Chan, M. H., Chang, M., Hou, Y. W., Chen, H. H, Hsu, H. R., and Lee, H. J. (2006). Arginine-rich intracellular delivery peptides noncovalently transport protein into living cells. *Biochem. Biophys. Res. Commun*., 346, 758–767.

[10] Liu, K., Lee, H. J., Leong, S. S., Liu, C. L., and Chou, C. J. (2007). A bacterial indole-3-acetyl-L-aspartic acid hydrolase inhibits mung bean (*Vigna radiata* L.) seed germination through arginine-rich intracellular delivery. *J. Plant Growth Regul*., 26, 278–284.

[11] Chang, M., Chou, J. C., Chen, C. P., Liu, B. R., and Lee, H. J. (2007). Noncovalent protein transduction in plant cells by macropinocytosis. *New Phytol*., 174, 46–56.

[12] Hou, Y. W., Chan, M. H., Hsu, H. R., Liu, B. R., Chen, C. P., Chen, H. H., and Lee, H. J. (2007). Transdermal delivery of proteins mediated by non-covalently associated arginine-rich intracellular delivery peptides. *Exp. Dermatol*., 16, 999–1006.

[13] Liu, B. R., Chou, J. C. and Lee, H. J. (2008). Cell membrane diversity in noncovalent protein transduction. *J. Membr. Biol*., 222, 1–15.

[14] Hu, J. W., Liu, B. R., Wu, C. Y., Lu, S. W., and Lee, H. J. (2009). Protein transport in human cells mediated by covalently and noncovalently conjugated arginine-rich intracellular delivery peptides. *Peptides*, 30, 1669–1678.

[15] Lu, S. W., Hu, J. W., Liu, B. R., Lee, C. Y., Li, J. F., Chou, J. C., and Lee, H. J. (2010). Arginine-rich intracellular delivery peptides synchronously deliver covalently and noncovalently linked proteins into plant cells. *J. Agricult. Food Chem*., 58, 2288–2294.

[16] Li, J. F., Huang, Y., Chen, R. L., and Lee, H. J. (2010). Induction of apoptosis by gene transfer of human *TRAIL* mediated by arginine-rich intracellular delivery peptides. *Anticancer Res*., 30, 2193–2202.

[17] Liou, J. S., Liu, B. R., Martin, A. L., Huang, Y. W., Chiang, H. J., and Lee, H. J. (2012). Protein transduction in human cells is enhanced by cell-penetrating peptides fused with an endosomolytic HA2 sequence. *Peptides*, 37, 273–284.

[18] Liu, B. R., Huang, Y. W., Chiang, H. J., and Lee, H. J. (2013). Primary effectors in the mechanisms of transmembrane delivery of arginine-rich cell-penetrating peptides. *Adv. Stu. Biol*., 5, 11–25.

[19] Liu, B. R., Huang, Y. W., and Lee, H. J. (2013) Mechanistic studies of intracellular delivery of proteins by cell-penetrating peptides in cyanobacteria. *BMC Microbiol*., 13, 57.

[20] Chen, C. P., Chou, J. C., Liu, B. R., Chang, M., and Lee, H. J. (2007). Transfection and expression of plasmid DNA in plant cells by an arginine-rich intracellular delivery peptide without protoplast preparation. *FEBS Lett.*, 581, 1891–1897.

[21] Dai, Y. H., Liu, B. R., Chiang, H. J., and Lee, H. J. (2011). Gene transport and expression by arginine-rich cell-penetrating peptides in *Paramecium*. *Gene*, 489, 89–97.

[22] Lee, C. Y., Li, J. F., Liou, J. S., Charng, Y. C., Huang, Y. W., and Lee, H. J. (2011). A gene delivery system for human cells mediated by both a cell-penetrating peptide and a *piggyBac* transposase. *Biomaterials*, 32, 6264–6276.

[23] Chen, Y. J., Liu, B. R., Dai, Y. H., Lee, C. Y., Chan, M. H., Chen, H. H., and Lee, H. J. (2012). A gene delivery system for insect cells mediated by arginine-rich cell-penetrating peptides. *Gene*, 493, 201–210.

[24] Liu, B. R., Lin, M. D., Chiang, H. J., and Lee, H. J. (2012). Arginine-rich cell-penetrating peptides deliver gene into living human cells. *Gene*, 505, 37–45.

[25] Liu, M. J., Chou, J. C., and Lee, H. J. (2013) A gene delivery method mediated by three arginine-rich cell-penetrating peptides in plant cells. *Adv. Stu. Biol*., 5, 71–88.

[26] Liu, B. R., Liou, J. S., Chen, Y. J., Huang, Y. W., and Lee, H. J. (2013) Delivery of nucleic acids, proteins, and nanoparticles by arginine-rich cell-penetrating peptides in rotifers. *Mar. Biotechnol*., in press.

[27] Wang, Y. H., Hou, Y. W. and Lee, H. J. (2007). An intracellular delivery method for siRNA by an arginine-rich peptide. *J. Biochem. Biophys. Methods*, 70, 579–586.

[28] Wadia, J. S. and Dowdy, S. F. (2002). Protein transduction technology. *Curr. Opin. Biotechnol.*, 13, 52–56.

[29] Gump, J. M. and Dowdy, S. F. (2007). TAT transduction: the molecular mechanism and therapeutic prospects. *Trends Mol. Med.*, 13, 443–448.

[30] Liu, B. R., Li, J. F., Lu, S. W., Lee, H. J., Huang, Y. W., Shannon, K. B., and Aronstam, R. S. (2010). Cellular internalization of quantum dots noncovalently conjugated with arginine-rich cell-penetrating peptides. *J. Nanosci. Nanotechnol*., 10, 6534–6543.

[31] Liu, B. R., Huang, Y. W., Chiang, H. J., and Lee, H. J. (2010). Cell-penetrating peptide-functionized quantum dots for intracellular delivery. *J. Nanosci. Nanotechnol*., 10, 7897–7905.

[32] Xu, Y., Liu, B. R., Chiang, H. J., Lee, H. J., Shannon, K. B., Winiarz, J. G., Wang, T. C., Chiang, H. J., and Huang, Y. W. (2010). Nona-arginine facilitates delivery of quantum dots into cells via multiple pathways. *J. Biomed. Biotechnol*., 2010, 948543.

[33] Liu, B. R., Huang, Y. W., Winiarz, J. G., Chiang, H. J., and Lee, H. J. (2011). Intracellular delivery of quantum dots mediated by a histidine- and arginine-rich HR9 cell-penetrating peptide through the direct membrane translocation mechanism. *Biomaterials*, 32, 3520–3537.

[34] Liu, B. R., Chiang, H. J., Huang, Y. W., Chan, M. H., Chen, H. H., and Lee, H. J. (2013) Cellular internalization of quantum dots mediated by cell-penetrating peptides. *Pharm. Nanotechnol*., 1, 151–161.

[35] Huang, Y. W., Lee, H. J., Liu, B. R., Chiang, H. J., and Wu, C. H. (2013) Cellular internalization of quantum dots. *Methods Mol. Biol*., 991, 249–259.

[36] Liu, B. R., Liou, J. S., Huang, Y. W., Aronstam, R. S., and Lee, H. J. (2013) Intracellular delivery of nanoparticles and DNAs by IR9 cell-penetrating peptides. *PLoS One*, 8, e64205.

[37] Liu, B. R., Lo, S. Y., Liu, C. C., Chyan, C. L., Huang, Y. W., Aronstam, R. S., and Lee, H. J. (2013) Endocytic trafficking of nanoparticles delivered by cell-penetrating peptides comprised of nano-arginine and a penetration accelerating sequence. *PLoS One*, in press.

[38] Liu, B. R., Winiarz, J. G., Moon, J. S., Lo, S. Y., Huang, Y. W., Aronstam, R. S., and Lee, H. J. (2013) Synthesis, characterization and applications of **carboxylated and** polyethylene-glycolated bifunctionalized InP/ZnS quantum dots in cellular internalization mediated by cell-penetrating peptides. *Colloids Surf. B Biointerfaces*, in press.

[39] Wender, P. A., Galliher, W. C., Goun, E. A., Jones, L. R., and Pillow, T. H. (2008). The design of guanidinium-rich transporters and their internalization mechanisms. *Adv. Drug Deliv. Rev*., 60, 452–472.

[40] Perevedentseva, E., Cai, P. J., Chiu, Y. C., and Cheng, C. L. (2011). Characterizing protein activities on the lysozyme and nanodiamond complex prepared for bio applications. *Langmuir*, 27, 1085–1091.

[41] Hirose, H., Takeuchi, T., Osakada, H., Pujals, S., Katayama, S., Nakase, I., Kobayashi, S., Haraguchi, T., and Futaki, S. (2012). Transient focal membrane deformation induced by arginine-rich peptides leads to their direct penetration into cells. *Mol. Ther*., 20, 984–993.

[42] Mattoussi, H., Palui, G. and Na, H. B. (2012). Luminescent quantum dots as platforms for probing in vitro and in vivo biological processes. *Adv. Drug Deliv. Rev*., 64, 138–166.

[43] Chen, F. and Gerion, D. (2004). Fluorescent CdSe/ZnS nanocrystal-peptide conjugates for long-term, nontoxic imaging and nuclear targeting in living cells. *Nano Lett*., 4, 1827–1832.

[44] Michalet, X., Pinaud, F. F., Bentolila, L. A., Tsay, J. M., Doose, S., Li, J. J., Sundaresan, G., Wu, A. M., Gambhir, S. S., and Weiss, S. (2005). Quantum dots for live cells, in vivo imaging, and diagnostics. *Science*, 307, 538–544.

[45] Mora-Huertas, C. E., Fessi, H. and Elaissari, A. (2010). Polymer-based nanocapsules for drug delivery. *Int. J. Pharm*., 385, 113–142.

[46] Webster, A., Compton, S. J. and Aylott, J. W. (2005). Optical calcium sensors: development of a generic method for their introduction to the cell using conjugated cell penetrating peptides. *Analyst*, 130, 163–170.

[47] Shu, S., Zhang, X., Teng, D., Wang, Z., and Li, C. (2009). Polyelectrolyte nanoparticles based on water-soluble chitosan-poly(L-aspartic acid)-polyethylene glycol for controlled protein release. *Carbohydr. Res*., 344, 1197–1204.

[48] Hunter, R. J. (1981). *Zeta Potential in Colloid Science*. London: Academic Press.

[49] Costa, A. L., Galassi, C. and Greenwood, R. (1999). Alpha-alumina-H_2O interface analysis by electroacoustic measurements. *J. Colloid Interface Sci*., 212, 350–356.

[50] Hanaor, D., Michelazzi, M., Leonelli, C., and Sorrell, C. C. (2012). The effects of carboxylic acids on the aqueous dispersion and electrophorestic deposition of ZrO_2. *J. Eur. Ceram. Soc*., 32, 235–244.

[51] Van Nieuwenhuyzen, W. and Szuhaj, B. F. (1998). Effects of lecithins and proteins on the stability of emulsions. *Eur. J. Lipid Sci. Technol*., 100, 282–291.